ACS Catalysis

Research Article

Cite This: ACS Catal. 2019, 9, 3849−3857

pubs.acs.org/acscatalysis

Ni−O Cooperation versus Nickel(II) Hydride in Catalytic Hydroboration of *N*-Heteroarenes

Jianguo Liu,[†] Jia-Yi Chen,[‡] Mengjing Jia,[†] Bangrong Ming,[†] Jiong Jia,[†] Rong-Zhen Liao,*[,‡] Chen-Ho Tung,[†] and Wenguang Wang*[,†]

[†]Key Lab of Colloid and Interface Chemistry, Ministry of Education, School of Chemistry and Chemical Engineering, Shandong University, No. 27 South Shanda Road, Jinan 250100, P.R. China

[‡]School of Chemistry and Chemical Engineering, Huazhong University of Science and Technology, 1037 Luoyu Road, Wuhan 430074, China

Supporting Information

ABSTRACT: An air-stable half-sandwich nickel(II) complex bearing a phosphinophenolato ligand, Cp*Ni(1,2-$Ph_2PC_6H_4O$) (**1**), has been designed and synthesized for activation of HBpin and catalytic hydroboration of *N*-heteroarenes such as pyridine. Through addition of the H−B bond across the Ni−O bond, **1** reacts with HBpin to afford an 18-electron Ni(II)−H intermediate [H**1**(Bpin)] featuring an oxygen-stabilized boron moiety, which readily reduces pyridine analogues to give the 1,2-hydroborated product, thus accomplishing the catalytic cycle under mild conditions. The necessity of the phosphinophenolato ligand to deliver the boryl group was manifested by the clear difference in the activity of **1** and Cp*NiH(PPh_3) (**3H**) in catalytic hydroborations. The latter lacks a functional oxygen atom and is inert to process the catalysis.

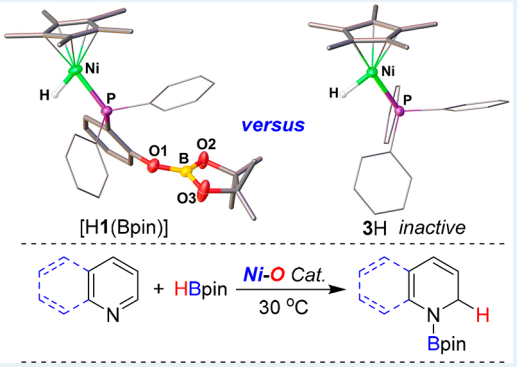

KEYWORDS: *metal−ligand cooperation, nickel(II) catalyst, B−H bond cleavage, nickel hydride, hydroboration*

INTRODUCTION

Catalytic reduction of six-membered *N*-heteroarenes through hydrogenation,[1] hydrosilylation, or hydroboration[2] has attracted continuous interest because the resultant dearomatized azacyclic compounds are important structural features of many biologically active compounds and pharmaceutical drugs.[3] The simplest partially reduced *N*-heteroarenes, 1,4-dihydropyridines, for example, are reminiscent of the reduced state of nicotinamide cofactor processing energy storage and release by enzymes, and these compounds are also valuable organic reducing agents for sustainable synthesis.[4] Compared to catalytic hydrogenation of *N*-heteroarenes, the reduction achieved through hydrosilylation or hydroboration by transition-metal catalysts or metal-free organocatalysts usually proceeds under relatively mild reaction conditions and achieves partial reductions with high regioselectivity.[2a,5]

In the context of transition-metal-catalyzed pyridine hydrosilylations or hydroborations, systems have been established using metal catalysts such as Ni,[6] Ru,[7−9] Mg,[10] and Zr[11] for the 1,4-reductions and Ca,[12] La,[13] Rh,[14] Ir,[15] Th,[16] Zn,[17] and Fe[18] for the 1,2-reductions. In most of these studies, a metal hydride (M−H) was considered to be a key intermediate.[7−19] It has been widely proposed that insertion of the C═N bond of a substrate into the M−H bond forming an amido−metal intermediate[9,12−19] or activation of the substrate can be achieved by abstracting the silicon cation from a hydrosilane σ complex[20−23] to generate M−H and N-silylpyridinium active species.[7] In addition to metal-centered catalysis, cooperative metal−ligand reactivity to activate the E−H bond providing M−H and silicon cations or borenium ions for catalytic reductions is unambiguously straightforward.[8,24−26] For example, the ruthenium−thiolate system has been reported to activate hydrosilanes, giving a Ru(II)−H species with the sulfur-stabilized silicon cation for 1,4-hydrosilylation of pyridines (Scheme 1, I).[8]

Metal−ligand cooperation is particularly useful in the design and exploration of efficient earth-abundant metal catalysts for homogeneous reductive transformations.[24] However, the challenge is tuning the Lewis acid−base coordination sphere interactions in an M---L system. It is difficult not only to activate the E−H bond (E = H, Si, or B) but also to generate the active species in a HM---L(E) fashion for the subsequent catalytic transformations.[24,25] We previously reported[27] an iron−thiolate system for exclusive 1,2-selective hydroboration of *N*-heteroarenes. Although the Fe−S bond is sufficiently polar to capture BH_3 and $(9\text{-BBN})_2$ to afford the stable iron−borane adduct, the activation of HBpin is endergonic and the catalysis is initiated by coordination of *N*-heteroarenes to the metal center.[18] In this paper, we describe a well-defined nickel(II)−oxygen cooperative catalyst bearing a phosphino-

Received: December 26, 2018
Revised: March 19, 2019
Published: March 20, 2019

DOI: 10.1021/acscatal.8b05136
ACS Catal. 2019, 9, 3849−3857

Scheme 1. Exploring Cooperative Metal−Ligand Catalyst for Pyridine Reduction[a]

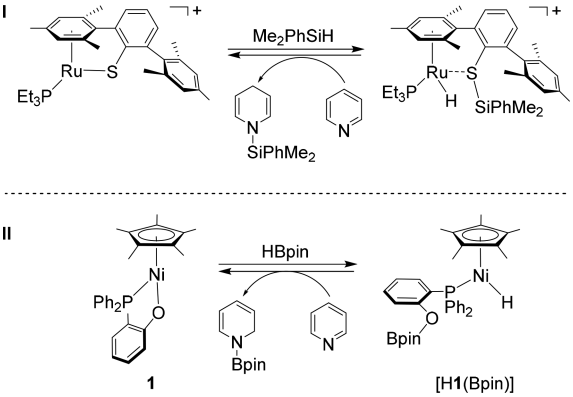

[a](I) Reported Ru−S system for catalytic hydrosilylation and (II) Ni−O system for catalytic hydroboration described in this work.

phenolato ligand that allows the activation of HBpin by direct addition of the H−B bond across the Ni−O bond (Scheme 1, II). The resultant 18-electron H−Ni(II)---O(Bpin) intermediate ([H**1**(Bpin)]) features an oxygen-stabilized boron moiety that is active for catalytic hydroboration of *N*-heteroarenes. In contrast, nickel(II) hydride Cp*NiH(PPh_3) (**3H**) without the functional oxygen site is inert as a catalyst.

RESULTS AND DISCUSSION

Synthesis and Characterization of Half-Sandwich Nickel Complexes. Cp*Ni(acac) was proven to be an optimal precursor for the synthesis of diverse half-sandwich nickel complexes.[28,29] The complexes Cp*Ni(1,2-$Ph_2PC_6H_4O$) (**1**) and Cp*Ni(1,2-$Ph_2PC_6H_4S$) (**2**) were conveniently synthesized by treatment of Cp*Ni(acac) with 1 equiv of 1,2-$Ph_2PC_6H_4ONa$ or 1,2-$Ph_2PC_6H_4SNa$ in tetrahydrofuran (THF), separately, at room temperature (Scheme 2). Both **1** and **2** are extremely air-stable compounds,

Scheme 2. Synthesis of Half-Sandwich Nickel(II) Complexes

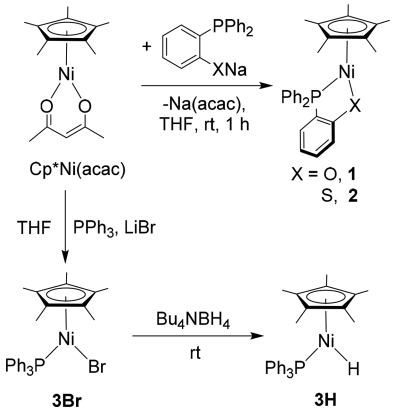

even in solution. The ^{31}P NMR spectrum of **1** exhibits a single resonance at δ 35.9 in C_6D_6, compared to that at δ 60.2 for **2**. By reacting with PPh_3 in the presence of LiBr, Cp*Ni(acac) was converted to Cp*NiBrPPh_3 (**3Br**), in which the Br^- ligand was further displaced by a hydride from Bu_4NBH_4, giving the nickel(II) hydride Cp*NiH(PPh_3) (**3H**, Scheme 2).[29] In the ^1H NMR spectrum, the hydride signal was observed at δ −20.06 (d, J_{P-H} = 98.3 Hz), corresponding to the phosphorus resonance at δ 52.2(s) observed in the ^{31}P NMR spectrum.

Crystallographic analysis confirmed the solid-state structures of **1** and **2**, which are neutral compounds exhibiting a similar framework of Cp*Ni(P−X) (Figure 1). The Ni−O distance of 1.891 (3) Å agrees well with 1.889 (2) Å reported for Cp*Ni(PEt_3)(OTol).[29b] Given the covalent atomic radii difference between S and O (Δr = 0.39 Å),[31] the difference of 0.289 Å between Ni−S (2.1798 (1) Å) and Ni−O (1.891 (3) Å) bonds implies a higher polarity of the Ni−O bond. Switching X from O to S causes the Cp*−Ni distance to increase from 1.737 to1.750 Å but decreases the Ni−P distance slightly (Δ(Ni−P) = 0.015 Å).

Activation of Hydroboranes. The polarity of Ni−X bonds in Cp*Ni(P−X) was demonstrated by the reactions with hydroboranes such as HBpin and $(9\text{-BBN})_2$ commonly used for hydroboration. We found that compound **2** is inactive toward HBpin and $(9\text{-BBN})_2$, whereas **1** is capable of activating HBpin and $(9\text{-BBN})_2$ to form the nickel(II) hydrides [H**1**(Bpin)] and [H**1**(BBN)] (eq 1). By treatment

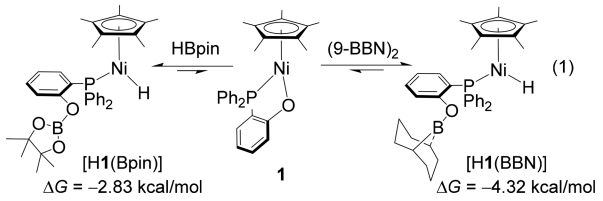

of a solution in benzene of **1** with excess (3 equiv) HBpin, the color of the solution turned from brown to deep red in several minutes. The ^{31}P NMR spectroscopic studies suggested that **1** was completely converted to [H**1**(Bpin)] with only a new ^{31}P signal displayed at δ 48.6 (s). When the reaction was conducted in C_6D_6, the ^1H NMR spectrum showed a characteristic hydride signal as a doublet at δ −20.28 (J_{P-H} = 99.0 Hz), consistent with the doublet at δ −20.06 (d, J_{P-H} = 98.3 Hz) observed for **3H**. The Ni−O complex also reacts readily with $(9\text{-BBN})_2$ to give [H**1**(BBN)] with a hydride resonance at δ −20.36 (d, J_{P-H} = 99.9 Hz) and the ^{31}P signal at δ 47.3 (s). No ^{11}B coupling with the hydride nuclei was observed, indicating complete B−H bond cleavage.[24c,26] Slow diffusion of hexane into the reaction solutions at −30 °C provided single crystals suitable for X-ray diffraction.

In the solid-state structures of [H**1**(Bpin)] and [H**1**(BBN)], the B−H bonds of HBpin and $(9\text{-BBN})_2$ were added across the Ni−O bond to retain a 18-electron configuration in the Cp*NiH(P−O(BR_2)) pattern (Figure 2). The $Me_5C_5^-$ ring and the P atom are coordinated to the Ni(II) center while the O atom is uncoordinated and connected to the boryl moiety. The hydride ligands were located and their positions were refined. Consistent with the NMR assignments, the hydride ligands in [H**1**(Bpin)] and [H**1**(BBN)] do not interact with the boron atoms. The Ni−H distances of 1.37 (8) Å for [H**1**(Bpin)] and 1.39 (5) Å for [H**1**(BBN)] are comparable to 1.37(3) Å reported for [$(Ph_2PCH_2C(CF_3)_2O)$NiH(PCy_3)][30] and 1.46 (3) Å for Cp*NiH(PEt_3)[29c] but shorter than the 1.52 (4) Å observed for **3H** (Figure 2).

Interestingly, the cleavage of the B−H bonds at the Ni−O site is reversible. For instance, when the crystals of [H**1**(Bpin)] were dissolved in benzene, the solution exhibits both **1** and [H**1**(Bpin)] as identified in its ^{31}P NMR spectrum. An equilibrium was alternatively established from the stoichiometric reaction of **1** with HBpin in benzene, which provided an

DOI: 10.1021/acscatal.8b05136
ACS Catal. 2019, 9, 3849−3857

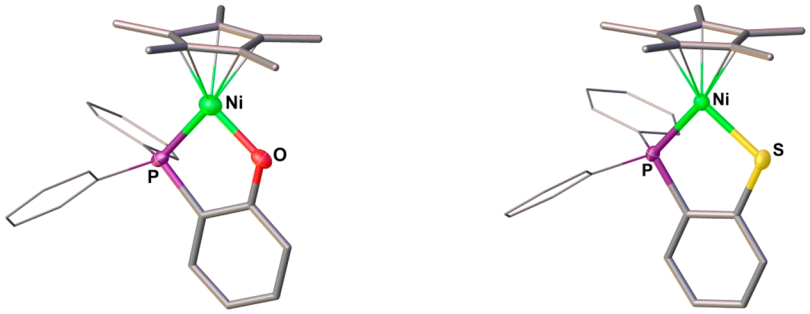

Figure 1. Structures of **1** (left) and **2** (right) with 50% probability thermal ellipsoids. For clarity, hydrogen atoms are omitted, and the two phenyl groups bonded at the phosphorus atom are drawn as lines. Selected bond distances (Å) and angles (deg): For **1**, Ni−O 1.891 (3), Ni−P 2.1290 (1), Ni−Cp*(centroid) 1.737, O−Ni−P 89.93 (8); for **2**, Ni−S 2.1798 (1), Ni−P 2.1140 (1), Ni−Cp*(centroid) 1.750, S−Ni−P 91.64 (4).

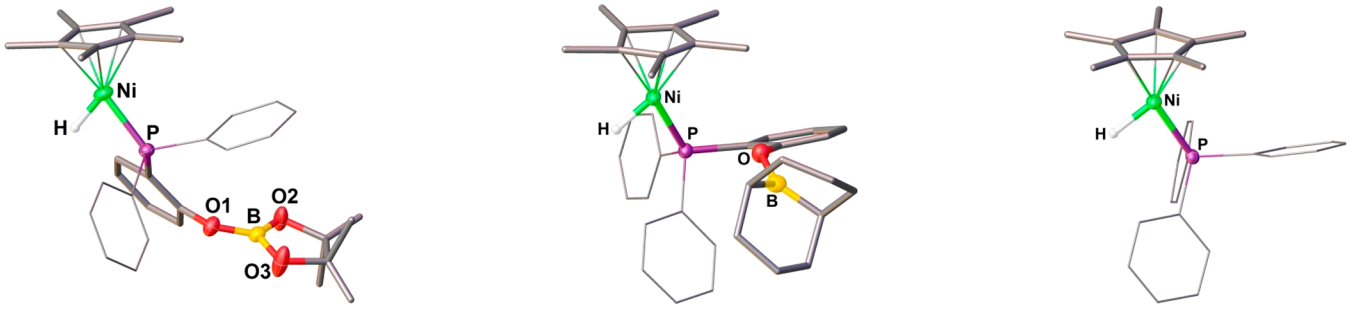

Figure 2. Structures of [H**1**(Bpin)] (left), [H**1**(BBN)] (middle), and **3**H (right) with 50% probability thermal ellipsoids. Selected bond distances (Å): For [H**1**(Bpin)], Ni−H 1.37 (8), Ni−P 2.0953 (2), O (1)−B 1.379 (8); for [H**1**(BBN)], Ni−H 1.39 (5), Ni−P 2.0888 (1), O (1)−B 1.372 (6); for **3**H, Ni−H 1.52 (4), Ni−P, 2.0856 (8).

equilibrium mixture of **1** and [H**1**(Bpin)] in a ratio of 1:2.74 determined by ^{31}P NMR spectra (Figure 3). The free energy

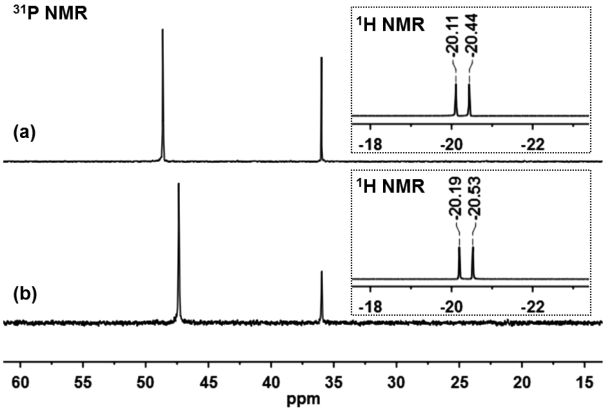

Figure 3. ^{31}P NMR spectra for the reactions of **1** with (a) 1 equiv of HBpin and (b) 0.5 equiv of $(9\text{-BBN})_2$. Inserts: ^{1}H NMR spectra of the hydride signals for [H**1**(Bpin)] and [H**1**(BBN)].

change (ΔG) for the addition of HBpin to **1** was estimated to be −2.83 kcal/mol according to the calculated equilibrium constant (K_{eq}^{θ} = 119.2). A similar equilibrium has also been established for $(9\text{-BBN})_2$ with **1** ($K_{eq}^{\theta} = 1.47 \times 10^3$), and the value of ΔG was estimated to be −4.32 kcal/mol (Figures S1 and S2). Such a reversible binding mode for the B−H bond activation at metal−ligand site resembles that reported for the Ru−S system.[24c]

Hydroboration of Pyridines. The catalytic activities of the nickel complexes in the hydroboration of pyridine were examined subsequently (Table S1, Supporting Information). Compound **1** was found to be an efficient catalyst for the hydroboration. At a loading of 2 mol % of **1** in C_6D_6, pyridine (**4a**) was hydroborated to afford a quantitative yield of *N*-borylated dihydropyridines within 6 h at 30 °C (Table S1, entry 3). Changing the borane reagent to $(9\text{-BBN})_2$ causes the conversion to the dihydropyridines to drop to 22%, even after a prolonged reaction time of 24 h. No hydroboration occurs in 24 h in the absence of **1**, showing that the Ni−O complex is responsible for the catalysis. By contrast, the Ni−S complex **2** and the Ni−H complex **3**H do not promote the hydroboration reaction, and the *N*-borylated dihydropyridines were not detected when **2** or **3**H was employed for the reaction of pyridine with HBpin or $(9\text{-BBN})_2$.

For Ni−O catalyzed pyridine hydroboration with HBpin, two *N*-borylated products, the 1,2- and 1,4-dihydropyridine isomers (**5a** and **5a**′, eq 2), were obtained. Monitored by ^{1}H

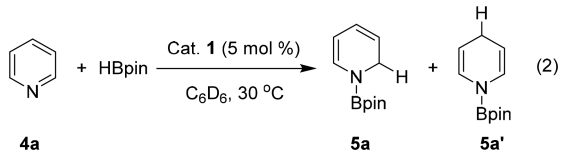

NMR spectra, the ratio of **5a**/**5a**′ was found to vary with time during the reaction (Figure 4). Kinetic analysis suggests that pyridine was completely hydroborated within 5 h, but the conversion of 1,2-product to 1,4-isomer proceeded slowly after the hydroboration (Figure 4). The ratio of **5a**/**5a**′ varied from 71/29 at 5 h to 53/47 after 29 h. The 1,4-dihydropyridine is thermodynamically more stable than 1,2-dihydropyridine[32] but 1,2-regioselective hydroboration of pyridine has been achieved using transition-metal catalysts.[12−18] In the present case, we propose that the Ni−O complex catalyzes the transformation

DOI: 10.1021/acscatal.8b05136
ACS Catal. 2019, 9, 3849−3857

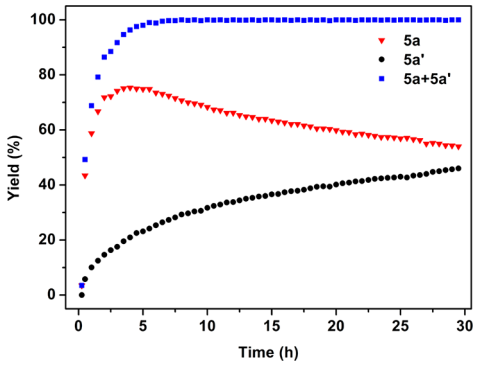

Figure 4. Yields of *N*-borylated dihydropyridines: 1,2-dihydropyridine pyridine (**5a**) and the 1,4-dihydropyridine (**5a′**) over time in the reaction of pyridine with HBpin catalyzed by **1** at 25 °C.

of the 1,2-hydroborated product to the 1,4-isomer (Figures S6 and S7). In particular, this transformation is very dependent on [**1**] and also on the reaction temperature (Tables S2 and S3), but it is independent of the HBpin concentration (Table S4). With an increase of [**1**] from 0.5 to 4 mol %, the ratio of **5a**/**5a′** decreased from 71/29 to 42/58 over a course of 24 h. The conversion of **5a** to **5a′** was slow at 0 °C and the catalysis provided **5a**/**5a′** in a ratio of 87/13 after 24 h (Table S2). Effects such as catalyst loading, reaction time, and temperature on the production distribution of **5a**/**5a′** have also been found for Mg−H-based hydroborations.[19,33]

To investigate the scope of the substrates, substituted pyridines were subjected to hydroboration by HBpin (Table 1). Functional groups such as $-CF_3$, −Bpin, −OMe, and −COOMe were all found to be tolerated under the reaction conditions. Pyridines possessing electron-donating or -withdrawing groups in the *para*-position were exclusively hydroborated, forming the corresponding 1,2-dearomatized products (**5b**−**5f**) in moderate to excellent yields within 24 h. Electron-donating groups appear to accelerate the transformation (**5b**, **5c**). In particular, this catalytic protocol is compatible with the Bpin functional group, offering **5f** which is amenable to further selective functionalization. Although hydroboration of 3-methoxypyridine (**4g**) proved to be challenging for the Lewis acid borane $B(Me)Ar^F_2$,[5a] **4g** was regioselectively hydroborated in this reaction to the 1,2-reduced product (**5g**,) in 80% yield. In the hydroboration of *meta*-substituted substrates with the exception of 3-methoxypyridine, both the *N*-borylated 1,2- and 1,4-dihydropyridine were detected. Kinetics studies for reactions demonstrated both the *N*-borylated 1,2- and 1,4-dihydropyridines were produced during the hydroboration reaction, and a slow isomerization of the 1,2-product to the 1,4-isomer took place after hydroboration (Figures S8 and S9). Productions of two isomers suggest the possibility of two different pathways for the catalytic process (see DFT calculations, below). Steric hindrance plays a significant role, evidenced by the lack of hydroboration activity for *ortho*-substituted pyridines (**4l** and **4m**) under the same conditions. Halogen substituents such as Cl, Br, and I on the pyridine ring were found to impede the hydroboration, producing unidentified precipitates.[6] In the ^{31}P NMR spectra recorded for the reaction mixture, the phosphorus resonance of the Ni−O catalyst had disappeared.

The Ni−O compound also exhibits excellent activity in the regioselective hydroboration of benzofused *N*-heterocycles (Table 2). Hydroboration of quinoline, for example, proceeded

Table 1. Nickel(II)-Catalyzed Hydroboration of Pyridines[a]

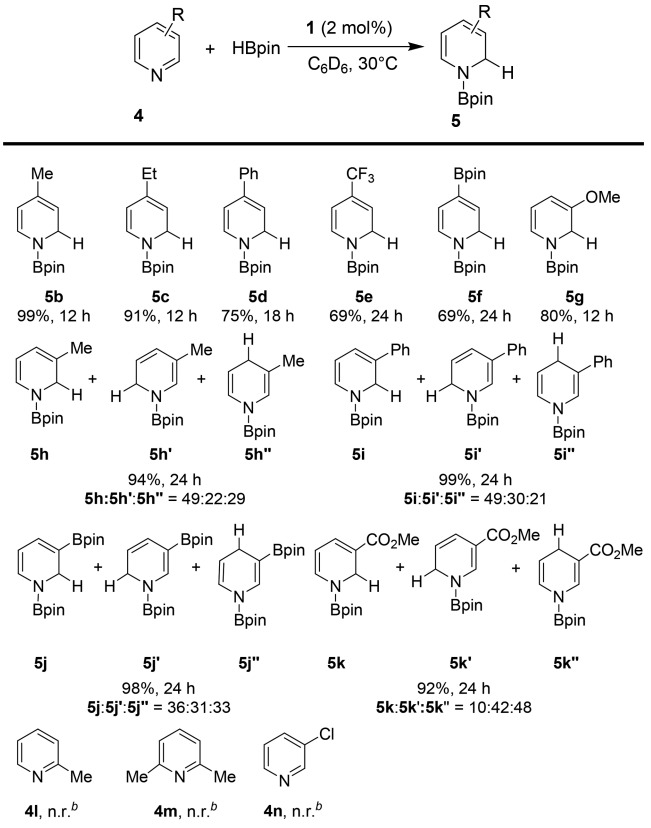

[a]Reaction conditions: pyridine substrates (0.3 mmol), HBpin (0.45 mmol), **1** (6 μmol, 2 mol %), and tetraethylsilane (0.03 mmol, internal standard) in 0.5 mL of C_6D_6. Yields determined by ^1H NMR spectroscopy are based on pyridines. [b]No reaction.

Table 2. Catalytic Hydroboration of *N*-Heterocyclic Compounds[a]

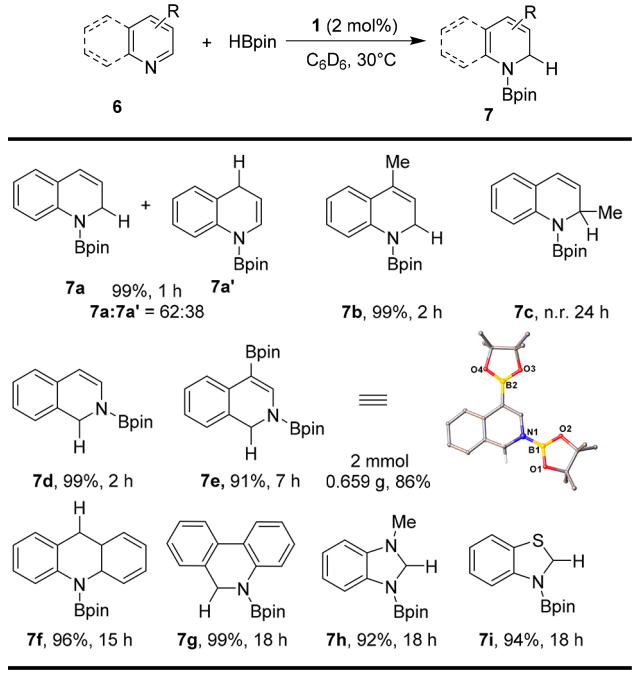

[a]Under the same reaction conditions as shown in Table 1.

DOI: 10.1021/acscatal.8b05136
ACS Catal. 2019, 9, 3849−3857

smoothly to completion within 1 h, giving the desired product in 99% yield with a **7a**/**7a**′ ratio of 62:38. Blocking the *para* position of an *N*-heterocyclic ring with a methyl group, as in 4-methylquinoline (**6b**), allows exclusive 1,2-reduction (**7b**, 99%). Hydroboration was not observed however for 2-methylquinoline, probably because of steric hindrance from the methyl group. Isoquinolines (**6d** and **6e**), acridine (**6f**), and phenanthridine (**6g**) are all regioselectively dearomatized under the mild reaction conditions, as demonstrated by the formation of **7d**−**7g** in high yields. Furthermore, Ni−O-catalyzed hydroboration was scaled up successfully without significant loss in efficiency as indicated by the reduction of **6e**, in which the 1,2-hydroborated product (**7e**), was isolated in 86% yield. The structure of **7e** was unambiguously confirmed by X-ray crystallographic analysis. This hydroboration approach is also available for the reduction of five-member *N*-heterocycles as exemplified by *N*-methylbenzimidazole (**6h**) and 1,3-benzothiazole (**6i**), with which HBpin was added to their C═N bonds selectively (**7h**, 92%, and **7i**, 94%).

Mechanistic Insights. To understand the catalytic hydroboration in depth, kinetic analyses were performed for hydroboration of 4-methylpyridine (**4b**) with HBpin catalyzed by **1** (eq 3). Performing the hydroboration with different

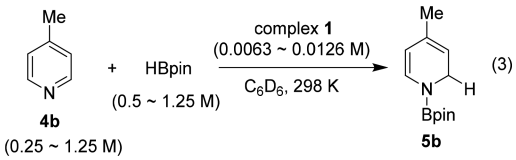

concentrations of the catalyst (0.0063−0.0126 M) led to a linear increase in the initial rate of the reaction (Figure 5a), indicating first-order kinetics in [**1**]. The initial rate of formation of **5b** was also found to linearly depend on [**4b**] but independent of [HBpin] (Figure 5b). These observations indicate that cleavage of the B−H bond is not the rate-limiting step in the catalytic reaction.

Density functional theory (DFT) calculations[34] were performed on the basis of the above elementary reactions. For the initial step of the catalysis, the free energy change ΔG, for the addition of HBpin to catalyst **1**, was calculated to be exergonic by 2.2 kcal/mol, which is in excellent agreement with the value estimated from the NMR experiments (ΔG = −2.83 kcal/mol). This free energy change is much less exergonic than the changes associated with the addition of $(9\text{-BBN})_2$ (ΔG = −9.5 kcal/mol) to **1**. In contrast, the addition of the B−H bonds across the Ni−S bond of **2** was found to be thermodynamically very unfavorable. These additions were calculated to be endergonic by 25.3 kcal/mol for HBpin and 13.3 kcal/mol for $(9\text{-BBN})_2$, respectively.

The DFT calculations showed that catalyst **1** has a very small singlet−triplet energy gap, although the nickel center has an 18-electron configuration. Specifically, the addition of HBpin to **1** was found to proceed via different pathways in the triplet and the singlet states. In the triplet state, the addition takes place in a stepwise manner, with the formation of $\mathbf{Int0}_{\mathbf{T}}$, a four-membered ring intermediate (Figure 6). The energy barriers for the first and second steps were calculated to be 8.9 and 11.3 kcal/mol, respectively. The formation of $\mathbf{Int1}_{\mathbf{T}}$ with the dissociation of the oxygen atom of the ligand from Ni is endergonic by 9.3 kcal/mol. In contrast, the addition of the B−H bond across the O−Ni bond in the singlet state is exergonic by 2.2 kcal/mol, and the barrier of 22.1 kcal/mol for $\mathbf{TS1}_{\mathbf{S}}$ is much higher than that for $\mathbf{TS1}_{\mathbf{T}}$. Consequently, the addition prefers to begin in the triplet state, and a spin crossing from triplet to singlet takes place during the formation of **Int1** ([H**1**(Bpin)]).

From **Int1**, three plausible mechanistic scenarios can be considered for the 1,2-addition. First, the pyridine substrate can coordinate to the boron atom of **Int1**, a step that was calculated to be endergonic by 8.7 kcal/mol. Then, the hydride in **Int2** transfers from the nickel center to the *ortho*-carbon of pyridine via $\mathbf{TS2}_{\mathbf{C2}}$ (Figure 7), and this is coupled with the coordination of the O atom to the nickel center. This process is associated with a barrier of 24.0 kcal/mol in the triplet state (31.2 kcal/mol in the singlet state) relative to **Int1** plus pyridine. $\mathbf{TS2}_{\mathbf{C2}}$ has been confirmed to be a true transition state with only one imaginary frequency of 279.5*i* cm^{-1}, which mainly corresponds to the hydride transfer. In $\mathbf{TS2}_{\mathbf{C2}}$, the scissile Ni−H1 bond is 1.60 Å, the nascent C1−H1 bond is 1.79 Å, and the Ni−O1 distance is 2.62 Å. The resulting intermediate $\mathbf{Int3}_{\mathbf{C2}}$ lies at +4.3 kcal/mol relative to **Int2**. During the reaction, the boron center functions as a Lewis acid to stabilize the pyridinium intermediate and the nickel center retains the 18-electron configuration from **Int2** to $\mathbf{Int3}_{\mathbf{C2}}$. In addition, the hydride transfer to the *para*-carbon has a much higher barrier (33.6 kcal/mol in the triplet state $\mathbf{TS2}_{\mathbf{C4}}$) because of geometric constraints. The final dissociation of the 1,2-product (**5a**) from the nickel complex via $\mathbf{TS3}_{\mathbf{C2}}$ has a barrier of only 3.2 kcal/mol relative to $\mathbf{Int3}_{\mathbf{C2}}$, and the whole

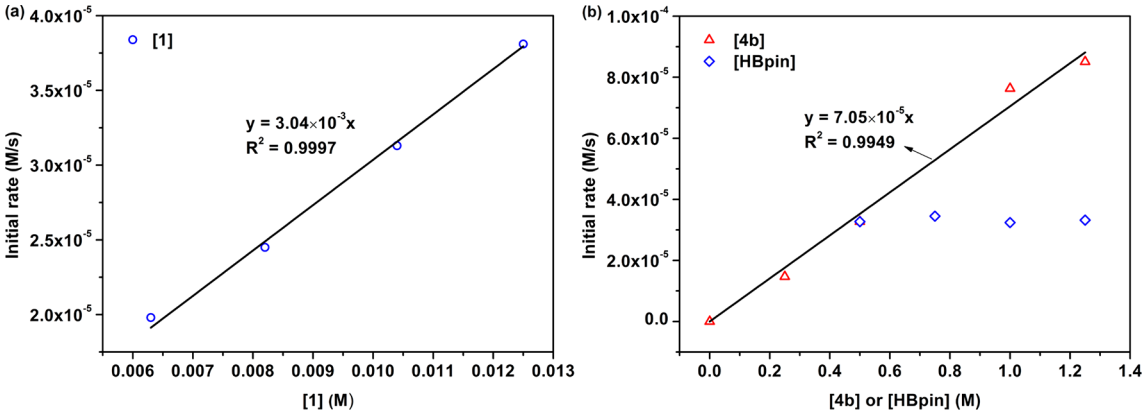

Figure 5. Kinetic analysis for hydroboration of 4-methylpridine in the presence of HBpin catalyzed by **1**: (a) plot of [**1**] (M) vs initial rate (M/s); (b) plots of [**4b**] and [HBpin] (M) vs initial rate (M/s).

DOI: 10.1021/acscatal.8b05136
ACS Catal. 2019, 9, 3849−3857

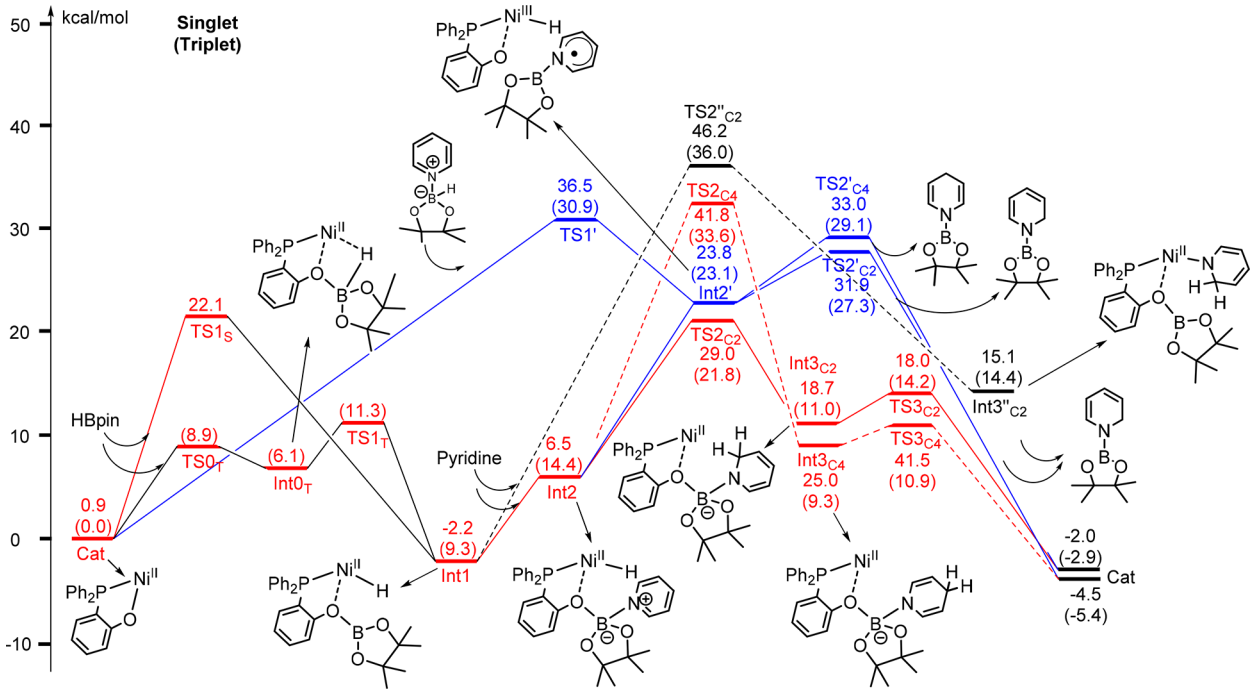

Figure 6. Gibbs free energy diagram (in kcal/mol) for the addition of HBpin to pyridine catalyzed by **1**. Schematic representations of all intermediates are shown. Energies in triplet state are given in brackets.

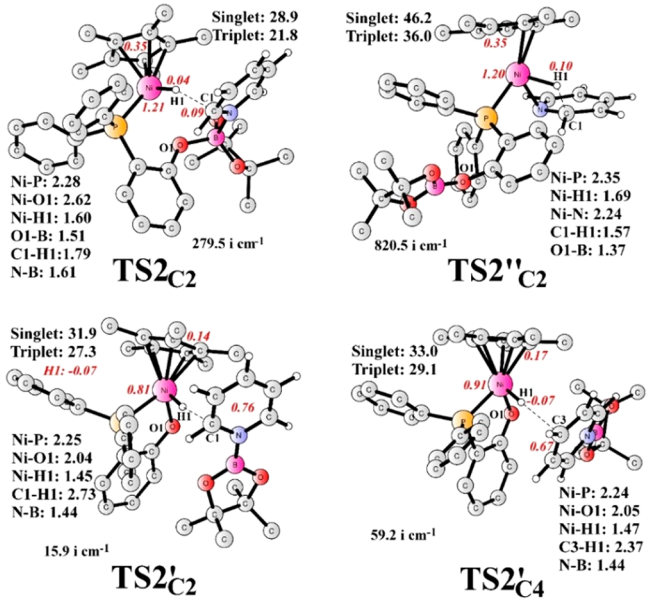

Figure 7. Structures of key transition states. For clarity, unimportant hydrogen atoms are not shown. Distances are given in angstroms, spin densities on selected atoms (groups) for the triplet state are shown in red italics, and the imaginary frequencies are also indicated.

reaction is exergonic by 2.9 kcal/mol. Hence, the 1,2-addition product is exclusively obtained via this pathway.

An alternative pathway based on **Int1** is through [2 + 2] addition of the Ni(II)−H to the C=N double bond of pyridine ($\mathbf{TS2''_{C2}}$, Figure 7). However, a barrier of 38.2 kcal/mol was predicted for the triplet state (48.4 kcal/mol in the singlet state) relative to **Int1** plus a pyridine molecule. A plausible reason for this high barrier is that $\mathbf{TS2''_{C2}}$ is in a 20-electron configuration. Such a high barrier rules out this [2 + 2] pathway as a viable option.

The third pathway is that **Int2** can be converted to a radical pair intermediate, **Int2′** by dissociation of the C_6H_5N---Bpin moiety from the phosphinophenolato oxygen of the nickel complex (ΔG = +16.6 kcal/mol). **Int2′** can be generated also by a hydrogen-atom transfer from the boron center of the C_6H_5N---HBpin complex to the nickel center of the catalyst via **TS1′** (blue curve in Figure 6). However, the barrier is found to be 30.9 kcal/mol in the triplet state, which is much higher than that in the first pathway. In **Int2′**, the hydrogen atom can be transferred from the nickel center to either the *ortho*-($\mathbf{TS2'_{C2}}$) or the *para*-carbon ($\mathbf{TS2'_{C4}}$) of the pyridine moiety. These two transition states were optimized and shown in Figure 7. $\mathbf{TS2'_{C2}}$ has a barrier of 4.2 kcal/mol relative to **Int2′**, but the barrier for $\mathbf{TS2'_{C4}}$ is 1.8 kcal/mol higher. Consequently, the formation of the 1,2-product by this pathway is kinetically more favorable. However, the formation of the 1,4-product is thermodynamically more favorable (exergonic by 5.4 kcal/mol for 1,4-addition and 2.9 kcal/mol for 1,2-addition). These calculated results support our hypothesis that the 1,2-product was produced initially and was converted to the 1,4-product, a conversion which is catalyzed by the nickel catalyst. The total barrier for such a conversion is 32.0 kcal/mol, which seems to be slightly overestimated. Because of the hydrogen-atom transfer nature of $\mathbf{TS2'_{C4}}$, however, the barrier should be lowered by several kcal/mol upon consideration of the quantum tunneling effect.

On the basis of the experimental and DFT studies, we propose a cooperative Ni−O-based cycle for pyridine hydroboration (Scheme 3). The catalytic reaction starts with B−H bond activation by **1**, generating the nickel(II) hydride [H**1**(Bpin)] with an oxygen-stabilized boron moiety. Although M−H species are envisioned to be the key active intermediates in catalytic hydroborations and hydrosilylations,[9−17,19,29] insertion of the C=N bond of *N*-heteroarenes into the Ni−H bond of [H**1**(Bpin)] to access amido−nickel intermediates is susceptible. The stoichiometric reaction of **3**H with pyridine

DOI: 10.1021/acscatal.8b05136
ACS Catal. 2019, 9, 3849−3857

Scheme 3. Proposed Catalytic Cycle for Hydroboration of Pyridine by the Ni−O Cooperative Catalyst

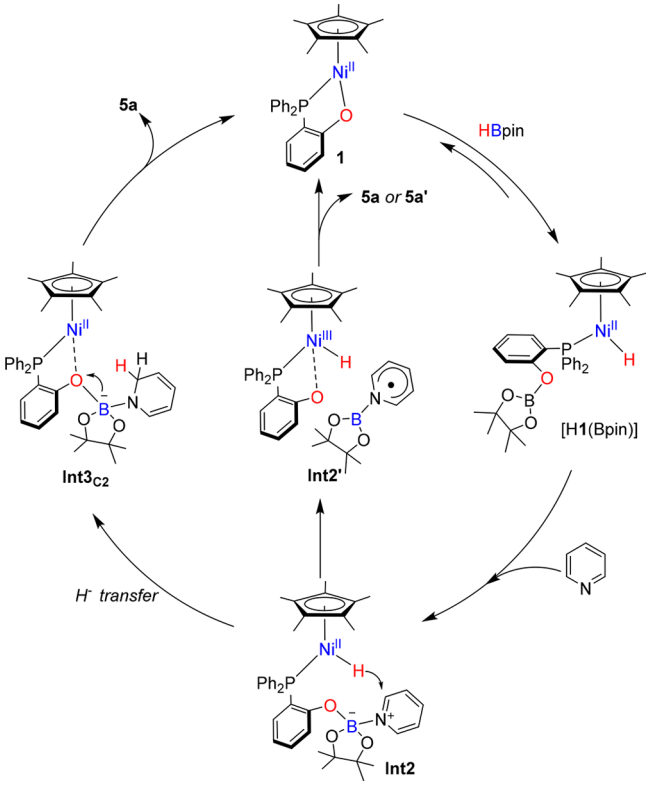

or 4-methylpyridine (eq 4, Figures S21−S25) has not in fact been observed, and in particular, **3H** is incapable of catalyzing

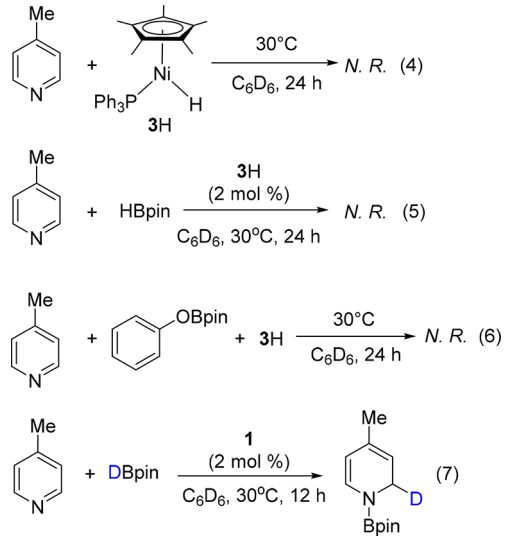

the hydroboration (eq 5). Especially, the production of **5b** was not observed for the reaction of 4-methylpyridine, **3H**, and PhOBpin. These results reflect the significance of cooperative Ni−O reactivity for catalytic hydroboration (eq 6, Figure S26).

For the reaction of [H**1**(Bpin)] with the pyridine, the path of coordination of the substrate with the boron atom of **Int1** is more thermodynamically favored than the insertion of C═N bond into the Ni−H bond. Subsequent transfer of the hydride from the nickel center to the *ortho*-carbon of pyridine in **Int2** results in formation of the intermediate **Int3**$_{C2}$, and is followed by the cleavage of the O−B bond to release the 1,2-hydroborated product regenerating the catalyst. Experimental isotope labeling result obtained from catalytic reduction of **4b** with deuterated pinacolborane (DBpin) verifies that the hydride is transferred to the *ortho*-carbon (eq 7, Figures S28 and S29).

CONCLUSIONS

We report an efficient air-stable cooperative Ni−O catalyst for the hydroboration of *N*-heteroarenes under mild conditions. The essential step of this Ni−O cooperative transformation is addition of the B−H bond of HBpin across the Ni−O bond, generating an active nickel(II) hydride with an oxygen-stabilized boron moiety. Kinetic analysis confirmed that the production of the 1,2-hydroborated product is more kinetically favored than production of the 1,4-isomer. DFT studies agree with the hypothesis that conversion of 1,2-product to the 1,4-product is catalyzed by the Ni−O catalyst via a radical-type mechanism. Despite the fact that many catalytic reductions involving nickel(II) hydrides have been delineated,[25d,35] the significant role of the phosphinophenolato site in delivering the boryl unit in hydroborations is manifested by the difference in catalytic activity of **1** and **3H**.

Cooperative metal−ligand reactivity in catalysis indeed can expand the applications of earth-abundant metals for homogeneous transformations. It should be noted that examples of catalytic selective reduction of pyridines using base-metal catalysts remain rare. In addition to our Fe−S system,[18,27] Findlater and co-workers recently reported[6] a convenient Ni(acac)$_2$/PCyp$_3$ system for regioselective 1,4-hydroboration of *N*-heteroarenes at 50 °C. In cases of this sort, the catalysis is initiated by binding the substrate to the metal center. In the context of cooperative abundant-metal−ligand reactivity for catalysis, the present Ni−O complex is the only case that covers reduction of pyridines. Recalling the challenge of tuning the Lewis acid−base coordination sphere interactions in a M---L system, the Ni−O and the Co−N system[24g] as well can activate the B−H bond for the hydroborations, but the Ni−S complex is inactive.

ASSOCIATED CONTENT

Supporting Information

The Supporting Information is available free of charge on the ACS Publications website at DOI: 10.1021/acscatal.8b05136.

Experimental details, characterization of the products, crystal data, and computational details (PDF)

Crystallographic data (CIF)

AUTHOR INFORMATION

Corresponding Authors

*E-mail: wwg@sdu.edu.cn (W.G.W.).
*E-mail: rongzhen@hust.edu.cn (R.-Z.L.).

ORCID

Rong-Zhen Liao: 0000-0002-8989-6928
Chen-Ho Tung: 0000-0001-9999-9755
Wenguang Wang: 0000-0002-4108-7865

Notes

The authors declare no competing financial interest.

DOI: 10.1021/acscatal.8b05136
ACS Catal. 2019, 9, 3849−3857

■ ACKNOWLEDGMENTS

We gratefully acknowledge the financial support from the "Thousand Plan" Youth Program and National Natural Science Foundation of China (21871166, 21873031, and 91427303).

■ REFERENCES

(1) (a) Bull, J. A.; Mousseau, J. J.; Pelletier, G.; Charette, A. B. Synthesis of Pyridine and Dihydropyridine Derivatives by Regio-and Stereoselective Addition to N-Activated Pyridines. *Chem. Rev.* **2012**, *112*, 2642−2713. (c) Paradies, J. Chiral Borane-Based Lewis Acids for Metal Free Hydrogenations. In *Topics in Organometallic Chemistry: Chiral Lewis Acids*; Mikami, K., Eds.; Springer: Berlin, 2018; Vol. *62*, pp 193−216.

(2) (a) Park, S.; Chang, S. Catalytic Dearomatization of N-Heteroarenes with Silicon and Boron Compounds. *Angew. Chem., Int. Ed.* **2017**, *56*, 7720−7738. (b) Meng, W.; Feng, X.; Du, H. Frustrated Lewis Pairs Catalyzed Asymmetric Metal-Free Hydrogenations and Hydrosilylations. *Acc. Chem. Res.* **2018**, *51*, 191−201.

(3) (a) Wender, P. A.; Schaus, J. M.; White, A. W. General Methodology for cis-Hydroisoquinoline Synthesis: Synthesis of Reserpine. *J. Am. Chem. Soc.* **1980**, *102*, 6157−6159. (b) Stout, D. M.; Meyers, A. I. Recent Advances in the Chemistry of Dihydropyridines. *Chem. Rev.* **1982**, *82*, 223−243. (c) Lavilla, R. Recent Developments in the Chemistry of Dihydropyridines. *J. Chem. Soc., Perkin Trans.* **2002**, *1*, 1141−1156. (d) Bull, J. A.; Mousseau, J. J.; Pelletier, G.; Charette, A. B. Synthesis of Pyridine and Dihydropyridine Derivatives by Regio-and Stereoselective Addition to N-Activated Pyridines. *Chem. Rev.* **2012**, *112*, 2642−2713. (e) Duttwyler, S.; Chen, S.; Lu, C.; Mercado, B. Q.; Bergman, R. G.; Ellman, J. A. Regio-and Stereoselective 1,2-Dihydropyridine Alkylation/Addition Sequence for the Synthesis of Piperidines with Quaternary Centers. *Angew. Chem., Int. Ed.* **2014**, *53*, 3877−3880. (f) Tejedor, D.; Cotos, L.; Mendez-Abt, G.; Garcia-Tellado, F. General Synthesis of Substituted 1,2-Dihydropyridines. *J. Org. Chem.* **2014**, *79*, 10655−10661.

(4) (a) Rueping, M.; Dufour, J.; Schoepke, F. R. Advances in Catalytic Metal-free Reductions: from Bio-Inspired Concepts to Applications in the Organocatalytic Synthesis of Pharmaceuticals and Natural Products. *Green Chem.* **2011**, *13*, 1084−1105. (b) Zheng, C.; You, S.-L. Transfer Hydrogenation with Hantzsch Esters and Related Organic Hydride Donors. *Chem. Soc. Rev.* **2012**, *41*, 2498−2518. (c) Ouellet, S. G.; Walji, A. M.; Macmillan, D. W. C. Enantioselective Organocatalytic Transfer Hydrogenation Reactions Using Hantzsch Esters. *Acc. Chem. Res.* **2007**, *40*, 1327−1339. (d) McSkimming, A.; Colbran, S. B. The Coordination Chemistry of Organo-Hydride Donors: New Prospects for Efficient Multi-Electron Reduction. *Chem. Soc. Rev.* **2013**, *42*, 5439−5488. (e) Chen, Q. A.; Chen, M. W.; Yu, C. B.; Shi, L.; Wang, D. S.; Yang, Y.; Zhou, Y. G. Biomimetic Asymmetric Hydrogenation: In Situ Regenerable Hantzsch Esters for Asymmetric Hydrogenation of Benzoxazinones. *J. Am. Chem. Soc.* **2011**, *133*, 16432−16435. (f) Chen, Q. A.; Gao, K.; Duan, Y.; Ye, Z. S.; Shi, L.; Yang, Y.; Zhou, Y. G. Dihydrophenanthridine: A New and Easily Regenerable NAD(P)H Model for Biomimetic Asymmetric Hydrogenation. *J. Am. Chem. Soc.* **2012**, *134*, 2442−2448.

(5) (a) Fan, X.; Zheng, J.; Li, Z. H.; Wang, H. Organoborane Catalyzed Regioselective 1,4-Hydroboration of Pyridines. *J. Am. Chem. Soc.* **2015**, *137*, 4916−4919. (b) Gandhamsetty, N.; Park, S.; Chang, S. Selective Silylative Reduction of Pyridines Leading to Structurally Diverse Azacyclic Compounds with the Formation of sp^3 C−Si Bonds. *J. Am. Chem. Soc.* **2015**, *137*, 15176−15184. (c) Keyzer, E. N.; Kang, S. S.; Hanf, S.; Wright, D. S. Regioselective 1,4-Hydroboration of Pyridines Catalyzed by an Acid-Initiated Boronium Cation. *Chem. Commun.* **2017**, *53*, 9434−9437. (d) Rao, B.; Chong, C. C.; Kinjo, R. Metal-Free Regio-and Chemoselective Hydroboration of Pyridines Catalyzed by 1, 3, 2-Diazaphosphenium Triflate. *J. Am. Chem. Soc.* **2018**, *140*, 652−656. (e) Hynes, T.; Welsh, E. N.; McDonald, R.; Ferguson, M. J.; Speed, A. W. Pyridine Hydroboration with a Diazaphospholene Precatalyst. *Organometallics* **2018**, *37*, 841−844.

(6) Tamang, S. R.; Singh, A.; Unruh, D. K.; Findlater, M. Nickel Catalyzed Regioselective 1,4-Hydroboration of N-Heteroarenes. *ACS Catal.* **2018**, *8*, 6186−6191.

(7) (a) Gutsulyak, D. V.; van der Est, A.; Nikonov, G. I. Facile Catalytic Hydrosilylation of Pyridines. *Angew. Chem., Int. Ed.* **2011**, *50*, 1384−1387. (b) Lee, S. H.; Gutsulyak, D. V.; Nikonov, G. I. Chemo-and Regioselective Catalytic Reduction of N-Heterocycles by Silane. *Organometallics* **2013**, *32*, 4457−4464.

(8) (a) Königs, C. D. F.; Klare, H. F.; Oestreich, M. Catalytic 1, 4-Selective Hydrosilylation of Pyridines and Benzannulated Congeners. *Angew. Chem., Int. Ed.* **2013**, *52*, 10076−10079. (b) Bähr, S.; Oestreich, M. A Neutral Ru^{II} Hydride Complex for the Regio-and Chemoselective Reduction of N-Silylpyridinium Ions. *Chem. - Eur. J.* **2018**, *24*, 5613−5622.

(9) (a) Kaithal, A.; Chatterjee, B.; Gunanathan, C. Ruthenium-Catalyzed Regioselective 1, 4-Hydroboration of Pyridines. *Org. Lett.* **2016**, *18*, 3402−3405.

(10) Mukherjee, D.; Shirase, S.; Spaniol, T. P.; Mashima, K.; Okuda, J. Magnesium Hydridotriphenylborate $[Mg(thf)_6][HBPh_3]_2$: A Versatile Hydroboration Catalyst. *Chem. Commun.* **2016**, *52*, 13155−13518.

(11) Ji, P.; Feng, X.; Veroneau, S. S.; Song, Y.; Lin, W. Trivalent Zirconium and Hafnium Metal−Organic Frameworks for Catalytic 1,4-Dearomative Additions of Pyridines and Quinolines. *J. Am. Chem. Soc.* **2017**, *139*, 15600−15603.

(12) Intemann, J.; Bauer, H.; Pahl, J.; Maron, L.; Harder, S. Calcium Hydride Catalyzed Highly 1, 2-Selective Pyridine Hydrosilylation. *Chem. - Eur. J.* **2015**, *21*, 11452−11461.

(13) Dudnik, A. S.; Weidner, V. L.; Motta, A.; Delferro, M.; Marks, T. J. Atom-Efficient Regioselective 1,2-Dearomatization of Functionalized Pyridines by An Earth-Abundant Organolanthanide Catalyst. *Nat. Chem.* **2014**, *6*, 1100−1107.

(14) Oshima, K.; Ohmura, T.; Suginome, M. Regioselective Synthesis of 1, 2-Dihydropyridines by Rhodium-Catalyzed Hydroboration of Pyridines. *J. Am. Chem. Soc.* **2012**, *134*, 3699−3702.

(15) Jeong, J.; Park, S.; Chang, S. Iridium-Catalyzed Selective 1,2-Hydrosilylation of *N*-Heterocycles. *Chem. Sci.* **2016**, *7*, 5362−5370.

(16) Liu, H.; Khononov, M.; Eisen, M. S. Catalytic 1,2-Regioselective Dearomatization of *N*-Heteroaromatics via A Hydroboration. *ACS Catal.* **2018**, *8*, 3673−3677.

(17) Lortie, J. L.; Dudding, T.; Gabidullin, B. M.; Nikonov, G. I. Zinc-Catalyzed Hydrosilylation and Hydroboration of *N*-Heterocycles. *ACS Catal.* **2017**, *7*, 8454−8459.

(18) Zhang, F.; Song, H.; Zhuang, X.; Tung, C.-H.; Wang, W. Iron-Catalyzed 1,2-Selective Hydroboration of *N*-Heteroarenes. *J. Am. Chem. Soc.* **2017**, *139*, 17775−17778.

(19) (a) Arrowsmith, M.; Hill, M. S.; Hadlington, T.; Kociok-Köhn, G.; Weetman, C. Magnesium-Catalyzed Hydroboration of Pyridines. *Organometallics* **2011**, *30*, 5556−5559. (b) Hill, M. S.; MacDougall, D. J.; Mahon, M. F. Magnesium Hydride-Promoted Dearomatisation of Pyridine. *Dalton Trans.* **2010**, *39*, 11129−11131. (c) Hill, M. S.; Kociok-Köhn, G.; MacDougall, D. J.; Mahon, M. F.; Weetman, C. Magnesium Hydrides and the Dearomatisation of Pyridine and Quinoline Derivatives. *Dalton Trans.* **2011**, *40*, 12500−12509.

(20) Park, S.; Brookhart, M. Hydrosilylation of Epoxides Catalyzed by a Cationic η^1-Silane Iridium (iii) Complex. *Chem. Commun.* **2011**, *47*, 3643−3645.

(21) (a) Gutsulyak, D. V.; Vyboishchikov, S. F.; Nikonov, G. I. Cationic Silane σ-Complexes of Ruthenium with Relevance to Catalysis. *J. Am. Chem. Soc.* **2010**, *132*, 5950−5951. (b) Mai, V. H.; Korobkov, I.; Nikonov, G. I. Half-Sandwich Silane σ-Complexes of Ruthenium Supported by NHC Carbine. *Organometallics* **2016**, *35*, 936−942.

(22) Corey, J. Y. Reactions of Hydrosilanes with Transition Metal Complexes. *Chem. Rev.* **2016**, *116*, 11291−11435.

DOI: 10.1021/acscatal.8b05136
ACS Catal. 2019, 9, 3849−3857

(23) Fuchs, J.; Klare, H. F.; Oestreich, M. Two-Silicon Cycle for Carbonyl Hydrosilylation with Nikonov's Cationic Ruthenium (II) Catalyst. *ACS Catal.* **2017**, *7*, 8338−8342.
(24) For selected examples on metal−ligand cooperative for activation of H−E (E = Si, B) in catalytic reaction. (a) Geri, J. B.; Szymczak, N. K. A Proton-Switchable Bifunctional Ruthenium Complex That Catalyzes Nitrile Hydroboration. *J. Am. Chem. Soc.* **2015**, *137*, 12808−12814. (b) Tseng, K.-N. T.; Kampf, J. W.; Szymczak, N. K. Modular Attachment of Appended Boron Lewis Acids to a Ruthenium Pincer Catalyst: Metal−Ligand Cooperativity Enables Selective Alkyne Hydrogenation. *J. Am. Chem. Soc.* **2016**, *138*, 10378−10381. (c) Stahl, T.; Müther, K.; Ohki, Y.; Tatsumi, K.; Oestreich, M. Catalytic Generation of Borenium Ions by Cooperative B−H Bond Activation: The Elusive Direct Electrophilic Borylation of Nitrogen Heterocycles with Pinacolborane. *J. Am. Chem. Soc.* **2013**, *135*, 10978−10981. (d) Drover, M. W.; Schafer, L. L.; Love, J. A. Capturing $HBCy_2$: Using N,O-Chelated Complexes of Rhodium(I) and Iridium(I) for Chemoselective Hydroboration. *Angew. Chem., Int. Ed.* **2016**, *55*, 3181−3186. (e) Drover, M. W.; Love, J. A.; Schafer, L. L. Toward anti-Markovnikov 1-Alkyne O-Phosphoramidation: Exploiting Metal−Ligand Cooperativity in a 1, 3-N, O-Chelated Cp* Ir (III) Complex. *J. Am. Chem. Soc.* **2016**, *138*, 8396−8399. (f) Chu, W. Y.; Zhou, X.; Rauchfuss, T. B. Cooperative Metal−Ligand Reactivity and Catalysis in Low-Spin Ferrous Alkoxides. *Organometallics* **2015**, *34*, 1619−1626. (g) Pang, M.; Wu, C.; Zhuang, X.; Zhang, F.; Su, M.; Tong, Q.; Tung, C.; Wang, W. Addition of a B−H Bond Across an Amido−Cobalt Bond: Co^{II}−H-Catalyzed Hydroboration of Olefins. *Organometallics* **2018**, *37*, 1462−1467.
(25) (a) van der Vlugt, J. I. Cooperative Catalysis with First-Row Late Transition Metals. *Eur. J. Inorg. Chem.* **2012**, *2012* (3), 363−375. (b) Morris, R. H. Exploiting Metal−Ligand Bifunctional Reactions in the Design of Iron Asymmetric Hydrogenation Catalysts. *Acc. Chem. Res.* **2015**, *48*, 1494−1502. (c) Zell, T.; Milstein, D. Hydrogenation and Dehydrogenation Iron Pincer Catalysts Capable of Metal−Ligand Cooperation by Aromatization/Dearomatization. *Acc. Chem. Res.* **2015**, *48*, 1979−1994. (d) Chakraborty, S.; Bhattacharya, P.; Dai, H.; Guan, H. Nickel and Iron Pincer Complexes as Catalysts for the Reduction of Carbonyl Compounds. *Acc. Chem. Res.* **2015**, *48*, 1995−2003. (e) Khusnutdinova, J. R.; Milstein, D. Metal−Ligand Cooperation. *Angew. Chem., Int. Ed.* **2015**, *54*, 12236−12273.
(26) Omann, L.; Königs, C. D. F.; Klare, H. F. T.; Oestreich, M. Cooperative Catalysis at Metal−Sulfur Bonds. *Acc. Chem. Res.* **2017**, *50*, 1258−1269.
(27) Song, H.; Ye, K.; Geng, P.; Han, X.; Liao, R.; Tung, C.-H.; Wang, W. Activation of Epoxides by a Cooperative Iron−Thiolate Catalyst: Intermediacy of Ferrous Alkoxides in Catalytic Hydroboration. *ACS Catal.* **2017**, *7*, 7709−7717.
(28) Bunel, E. E.; Valle, L.; Manriquez, J. M. Pentamethylcyclopentadienyl Acetylacetonate Complexes of Iron(II), Cobalt(II), and Nickel(II). Convenient Synthetic Entries to Mono-η^5-C_5Me_5 Derivatives. *Organometallics* **1985**, *4*, 1680−1682.
(29) (a) Holland, P. L.; Andersen, R. A.; Bergman, R. G. Synthesis, Characterization, Isomerization, and Reactivity of Dimeric Cyclopentadienylnickel Amido Complexes. *J. Am. Chem. Soc.* **1996**, *118*, 1092−1104. (b) Holland, P. L.; Andersen, R. A.; Bergman, R. G.; Huang, J.; Nolan, S. P. Monomeric Cyclopentadienylnickel Methoxo and Amido Complexes: Synthesis, Characterization, Reactivity, and Use for Exploring the Relationship between H-X and M-X Bond Energies. *J. Am. Chem. Soc.* **1997**, *119*, 12800−12814. (c) Holland, P. L.; Smith, M. E.; Andersen, R. A.; Bergman, R. G. X-ray Crystal Structures of $Cp^*Ni(PEt_3)X$ [X = Br, O(*p*-C_6H_4Me), NH(*p*-C_6H_4Me), S(*p*-C_6H_4Me), OCH_3, $CH_2C_6H_5$, Me, H, PEt_3^+]. Understanding Distortions and Trans Influences in Cyclopentadienyl Complexes. *J. Am. Chem. Soc.* **1997**, *119*, 12815−12823.
(30) Müller, U.; Keim, W.; Krüger, C.; Betz, P. [{$Ph_2PCH_2C(CF_3)_2O$}$NiH(PCy_3)$]: Support for A Nickel Hydride Mechanism in Ethene Oligomerization. *Angew. Chem., Int. Ed. Engl.* **1989**, *28*, 1011−1013.
(31) Cordero, B.; Gómez, V.; Platero-Prats, A. E.; Revés, M.; Echeverría, J.; Cremades, E.; Barragán, F.; Alvarez, S. Covalent Radii Revisited. *Dalton Trans.* **2008**, No. 21, 2832−2838.
(32) (a) Keay, J. G. The Reduction of Nitrogen Heterocycles with Complex Metal Hydrides. *Adv. Heterocycl. Chem.* **1986**, *39*, 1−77. (b) Fowler, F. W. Relative Stabilities of the N-Methyldihydropyridines. *J. Am. Chem. Soc.* **1972**, *94*, 5926−5927. (c) Eisner, U.; Kuthan, J. Chemistry of Dihydropyridines. *Chem. Rev.* **1972**, *72*, 1−42.
(33) Intemann, J.; Lutz, M.; Harder, S. Multinuclear Magnesium Hydride Clusters: Selective Reduction and Catalytic Hydroboration of Pyridines. *Organometallics* **2014**, *33*, 5722−5729.
(34) For computational details, see Supporting Information.
(35) Eberhardt, E. A.; Guan, H. Nickel Hydride Complexes. *Chem. Rev.* **2016**, *116*, 8373−8426.

DOI: 10.1021/acscatal.8b05136
ACS Catal. 2019, 9, 3849−3857